




Study of discharge and jump of water flow from water regulatory structures in channels

Zhuzbay Kassymbekov   Abai Shinibaev, Galimzhan Kassymbekov 

Satbayev University, Satpayev Str., 22, Almaty, 050013, Kazakhstan

RECEIVED 10.02.2021

ACCEPTED 16.08.2021

AVAILABLE ONLINE 08.06.2022

Abstract: One of the main causes of damage to weirs regulating the flow of water in canals is local erosion of the bottom and banks. This is mainly due to the excessive kinetic energy of the stream flow and the uneven volumetric distribution of the water flow rate at the end of the strengthening. Due to this, 35–40% of hydraulic structures fail prematurely. The aim of the research was to determine the parameters of the spatial hydraulic jump arising behind the hydrotechnical structure and the rapid expansion of the cross-section. The research showed that the hydraulic jump with a curved cylinder in the plan is a spatial form and not only dissipates the energy of the stream, but also acts as a diffuser. With the stream expansion angle values in the range of 7–10°, a highly turbulent flow remains, which still has high kinetic energy at a distance from the end of the structure. At an angle of 25–27°, the flow is smooth, the velocity distribution is uniform across the width of the channel. In some cases, the forced expansion of the cross-section at the outflow of the weir favours the energy dissipation and uniform flow velocity distribution.

Keywords: abrupt channel expansion, energy dissipation, hydraulic jump, open channel, spatial jump, water flow, weir

INTRODUCTION

As the materials of the European Environment Agency [EEA 2020] show, in all the Eastern Partnership countries, the bulk of water resources are consumed in agriculture and industrial enterprises, and 70% of water is used for irrigation.

The relationship between the water and energy sectors and their planning processes using assessment system software allows for alternative options for action [CARVALHO *et al.* 2019; ERSOY *et al.* 2021].

The construction of various hydraulic structures and hydroelectric power plants for the integrated use of water; and water energy has always been of great relevance. The results of the study show that the reliability of the reservoir and dams increases the stability of the water supply system of settlements [BOUSSEKINE *et al.* 2016; SUTHERLAND, SMITH 2018]. The efficiency of hydraulic structures directly depends on the reliability of construction and operation, including in the hydropower system [ZHURINOV *et al.* 2019; 2020]. Otherwise, they drastically reduce performance or quickly fail. The condition assessment model developed for this purpose includes the main technological parameters and qualities

[DE LEO *et al.* 2020]. In this regard, the results of the study of the technology of modernisation and efficient use, the contour instability of irrigation canals with variabwidths, as well as the prevention of coastal erosion deserve attention [REPETTO *et al.* 2002; ZHANG *et al.* 2013]. The study of the instability of the aquatic ecosystem expands the boundaries of traditional approaches in this matter [EL-HAZEK *et al.* 2020; TSKHAL, AGEIKOV 2021].

The reasons for the destruction of the channel of the earthen canals are primarily the concentrated discharge of the descending water and the presence of unsteady flow, especially during water distribution [ASHOOR, RIAZI 2019; WU *et al.* 2020].

Experiments and numerical analysis of water flow in an open canal confirm the influence of flow velocity profiles on the technical condition of the bottom of the canal [MICHALOLIAS *et al.* 2018].

It has been established that the normal functioning of water regulating structures is influenced by the stability of the channel, the velocity and turbulence of water flow and soil erosion [JONES, RICHARDSON 2004; RUSTIATI *et al.* 2017; SHINIBAEV 2010].

The analysis shows that by the beginning of the XXI century the state of mathematical and physical modelling of the complex

phenomenon of interaction of hydraulic structures with a stream and channel still requires further development [CLOPPER, LAGASSE 2011; RUSTIATI *et al.* 2017; SHEPPARD *et al.* 2004].

The following analysed works more closely correspond to the purpose of our article. They considered the cases of contact of a turbulent flow with a calm flow in the conditions of a plane problem.

The study results of the well-known cantilever and stepped spillways provide overload protection on earth and stone embankments and dissipate the energy of destruction [FRIZELL, FRIZELL 2015]. The use of porous screens to prevent the destruction of open channels with supercritical flow and Froude number also dissipates more energy compared to the reverse tilt [ABBASPOUR *et al.* 2019]. Two-dimensional turbulence in three-dimensional flows [XIA, FRENKIEL 2017] shows the presence of a reverse energy cascade in two different systems, namely flows in thick layers of liquid.

Due to the need to obtain materials for full-scale conditions, some works are devoted to the study of large-scale flow.

Here, the main attention is paid to the main features of the subcritical transition to turbulence, the study of the structure of the traveling wave type at the trailing edge of the turbulent flow and the asymmetric quadrupole centered at the point [LEMOULT *et al.* 2013; TREBICKA 2018].

Based on the study of the turbulent flow in a rectangular channel with inclined baffles, the pressure recovery coefficient along the channel wall was established [EL-ASKARY *et al.* 2013]. The article of DANIEL and PAULUS [2019] provides some recommendations for the rational management of accidents and failures of hydraulic structures, based on European and American practice.

In the article of OMID *et al.* [2007] of this population, a gradually expanding hydraulic jump in trapezoidal canals is considered. It noted that a decrease in the slope of the sidewalls for an assumed expansion angle causes a smaller subsequent depth and a longer jump length and energy loss.

The ratio of subsequent depths usually decreases with increasing divergence angles. However, with an increase in angles of more than 15°, it does not significantly affect this ratio [KASHEIPOUR, BAKHTIARI 2009]. For the range of Froude numbers from 2 to 4, the average decrease in this ratio for an angle of 25° was about 27%.

The issue of the length of a hydraulic jump in a non-prismatic channel is of great importance, since the length depends on the length of the water-carrying part of the structures and the parameters of the apron [BEGLYAROVA *et al.* 2018]. Analysis of

some experimental data shows that a negative slope of the channel decreases the subsequent depth ratio, and a positive slope increases the subsequent depth ratio [BEIRAMI, CHAMANI 2006].

It was found that when the cross-section coefficient $k_1 \approx 3$, the ratio of the hydraulic jump length reaches its maximum value [SADIQ 2007].

In general, the above analysis shows that the phenomena occurring in the tailwater junction area are more complex than in the conditions of the plane problem. This situation causes significant difficulty in calculating the main parameters of the spatial flow, which must be taken into account in order to protect the structure from coastal soil erosion. Due to the indicated complexity of the process, the task of determining the conjugate depths of a jump with a roller curved in plan has not yet had the required solution.

STUDY METHODS

GENERAL INFORMATION

When considering the process under study, the procedure for changing the forms of conjugation of the pits was adopted during the transition to a dry wide channel of rectangular section behind the structure [KASYMBEKOV, SHINIBAYEV 2009]. It is made of an open type of rectangular cross-section with a zero slope and without a threshold at the entrance.

The compression ratio of the flow in the plan was taken to be close to the boundary value, since in this case the characteristic features of the conjugation forms become sharply expressed.

$$\eta = \frac{b_0}{b_p} = 0.5 \quad (1)$$

where: b_0 = inlet flow width (cm), b_p = outlet flow width in the channel (cm).

In the theoretical study of the process of spatial flow jump, turbulent flow behind the structure, the basic moments of the law on the change in momentum, the Bernoulli equation, the Cardan formula were used, as well as the existing methods for calculating the conjugate depths of the considered jump.

The supply of water for the formation of a turbulent flow and a hydraulic jump in the experimental stand (Fig. 1, Photo 1) is provided by the outflow of the flow from under a shield (8) when it rises by 2–5 cm (gap). It also allows you to vary the depth of the stream to create a compressed jump. At the end of the process, the used water is returned to the reservoir through the

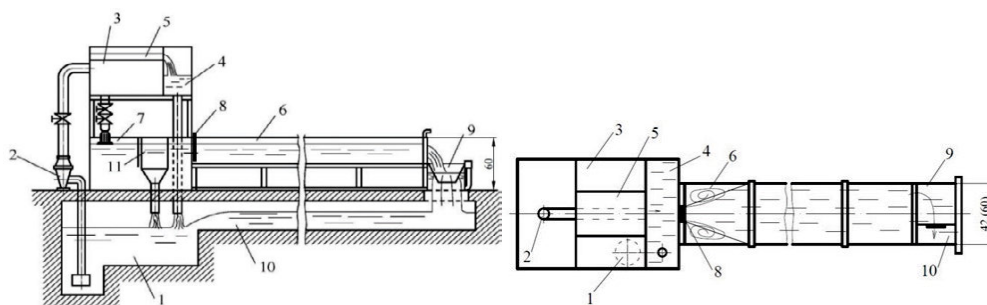


Fig. 1. Schematic of the experimental stand with trays; 1 = capacity; 2 = centrifugal pump; 3 = working compartment; 4 = assembled compartment; 5 = channel; 6 = large tray; 7 = small tray; 8 = shield; 9 = weir; 10 = channel backflow; 11 = funnel; source: KASYMBEKOV and SHINIBAYEV [2009]

weir (9) and the rear drain channel (10), which is laid under the floor. Excess water is drained into the reservoir using a funnel (11). At the same time, the flow rates on a large tray were measured with a Rebeck tube with a receiving part of 4 mm in diameter and an X-6 micro-spinner with a record on the H-700 oscillogram.



Photo 1. General view of the experimental stand – construction Dulat University (phot. A. Shinibayev)

Experiments on a small part of the stand were carried out with symmetric lateral compression of the flow (compression ratio $\eta = 0.4-0.8$) and a water flow rate in the range of $5-9 \text{ dm}^3 \cdot \text{s}^{-1}$.

At the same time, the measurement of the water flow rate in the open channel, the control of turbulent flows were carried out according to the method described in our previous work [SHINIBAEV 2010].

When studying the process, the outflow of the water regulating structure into the downstream was accompanied by the spread of a storm flow in the plan. The spreading symmetry was achieved when the axis of the channel and the structure coincided and the water depth was shallow. Due to the continuous planned expansion of the flow in this section, there was a decrease in depth and a corresponding increase in velocity.

Semi-free spreading was formed in the case when the extreme trickles of a stormy stream do not reach the width of the flume, and the side vortex areas are connected to a calm stream. At the same time, in the spreading zone a characteristic sheet was formed, limited on all sides, with the exception of the outlet section. The spreading angle α was determined by the formula [SHINIBAEV 2010]:

$$\text{tg}\alpha = \frac{\sqrt{gh_0}}{v} = \frac{1}{\sqrt{\text{Fr}_{20}}} \quad (2)$$

where: h_0 = flow depth in the outlet section 0-0 (cm); origin of coordinates ($x = 0, z = 0.04$); v = flow velocity in the outlet section 0-0 ($\text{m} \cdot \text{s}^{-1}$); Fr_{20} = Froude number at the exit from the structure.

During the experiments, the longitudinal and transverse components of the velocities changed with distance from the outlet section, and in accordance with this, the flow spreading coals changed. This led to the fact that the extreme streams, expanding in the flow plan, did not remain straight.

Visual observation of the process was accompanied by a sketch of the conjugation forms, the position of the spreading zones and eddies. The length of the rollers was recorded using coloured indicators. The marks of the bottom and water level in

the areas under study were measured with a measuring arrow, and the jump length – with a scale ruler and using an empirical formula [ABDURAMANOV 2010].

MATHEMATICAL MODELLING OF THE PROCESS

For the theoretical consideration (modelling) of the process as a whole and the hydraulic jump, a fluid compartment was adopted between two cylindrical sections I-I and II-II (Fig. 2) [MIKHALEV 2013].

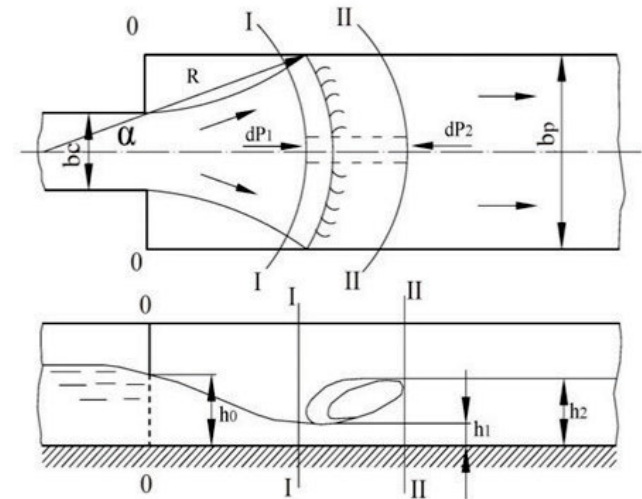


Fig. 2. Schematic of the spatial jump of the jet; R = jet deflection radius (cm), P_1 = impulse of acting forces in section I-I ($\text{N} \cdot \text{s}$), P_2 = impulse of acting forces in section II-II ($\text{N} \cdot \text{s}$), h_1 = depth at the beginning of the hydraulic jump (cm), h_2 = depth at the end of the hydraulic jump (cm), α = momentum indicator; source: KASSYMBEKOV and SHINIBAYEV [2009]

Based on the law of changing the momentum and neglecting the friction forces in the section between the sections under consideration, one can write [ABBASPOUR *et al.* 2019]:

$$\Delta K = \sum P \quad (3)$$

where: ΔK = increment in the amount of motion per unit of time, $\sum P$ = the sum of the projections of the impulses of all acting forces on the axis of symmetry ($\text{N} \cdot \text{s}$).

$$\sum P = dP_1 + dP_2 \quad (4)$$

In this case, the increment in the amount of motion is presented in the following form:

$$\Delta K = (\alpha_{02} \rho v_2^2 h_2 - \alpha_{01} \rho v_1^2 h_1) R d\theta \quad (5)$$

where: θ = angle (rad), $d\theta$ = average derivative of θ .

Average speeds v_1 and v_2 ($\text{m} \cdot \text{s}^{-1}$) in sections I-I and II-II are determined by of the Equation (6):

$$v_1 = \frac{Q}{h_1 R \theta}, v_2 = \frac{Q}{h_2 R \theta} \quad (6)$$

where: Q = water consumption ($\text{cm}^3 \cdot \text{s}^{-1}$), $R\theta$ = the length of the arc along which the curved section is drawn.

Taking into account that $\rho = \frac{\gamma}{g}$ and substituting the value of average velocities, we rewrite Equation (5) in the following form:

$$\Delta K = \frac{\gamma}{gR} \left(\frac{Q}{\theta} \right)^2 \left(\frac{\alpha_{01}}{h_1} - \frac{\alpha_{02}}{h_2} \right) d\theta \quad (7)$$

where: ρ = density of liquid ($\text{Mg}\cdot\text{m}^{-3}$); α_{01} , α_{02} = momentum coefficients in sections I-I and II-II.

$$\frac{h_1^2}{2} + \left(\frac{Q}{R\theta} \right)^2 \frac{\alpha_0}{gh_1} = \frac{h_2}{2} + \left(\frac{Q}{R\theta} \right)^2 \frac{\alpha_0}{gh_2} \quad (8)$$

where: α_0 = kinetic energy correction factor.

Solving this equation for conjugate depths will give the Equation (9):

$$h_1 = \frac{h_2}{2} \left(\sqrt{1 + \frac{8\alpha_0}{h_2^3 g} \left(\frac{Q}{R\theta} \right)^2} - 1 \right) \quad (9)$$

Substituting the values of ΔK , ΣP from Equations (7) and (4) into Equation (3), and after some transformation, and also assuming $\alpha_{01} = \alpha_{02} = \alpha_0$, we obtain the equation spatial jump:

$$dP_1 = \frac{\gamma h_1^2}{2} R d\theta \quad (10)$$

$$dP_2 = \frac{\gamma h_2^2}{2} R d\theta \quad (11)$$

where: P_1 = impulse of acting forces in section I-I (N·s), P_2 = impulse of acting forces in section II-II (N·s), γ = specific gravity of liquid ($\text{N}\cdot\text{m}^{-3}$), h_1 = depth at the beginning of the hydraulic jump (cm), h_2 = depth at the end of the hydraulic jump (cm), R = jet deflection radius (cm), $\theta = \frac{\alpha\pi}{90}$ = angle (rad).

The critical depth h_{cr} in curvilinear design sections is defined as:

$$h_{cr} = \sqrt[3]{\frac{\alpha_0}{g} \left(\frac{Q}{R\theta} \right)^2} \quad (12)$$

Hence, it can be seen that with a decrease in the degree of compression of the flow by the structure in the plan, the angle of expansion of the stormy flow before the jump decreases, the curvilinear design sections before and after the jump approach flat in shape, and in the complete absence of the planned compression of the flow, the equality $R\theta = B$ takes place.

In those cases when the water depth in the diversion channel is greater than the second conjugate depth of the spatial jump in the critical position, determined by Equation (9), the jump is flooded, which is accompanied by the appearance of other forms of conjugation of the bays.

In this case, the compressed depth before the jump h_1 with a sufficient degree of accuracy can be calculated based on the law of continuity, if the value of the average velocity in the compressed section v_1 is known:

$$h_1 = \frac{Q}{R\theta v_1} \quad (13)$$

From the Bernoulli equation for the exit section of the structure and the compressed section before the jump it follows that:

$$v_1 = \sqrt{2g \left(1 - \frac{h_1}{h_0} \right) h_0 + v_0^2} \quad (14)$$

Taking into account the above, we write Equation (13) in the following form:

$$h_1 = \frac{Q}{R\theta \sqrt{2g \left(1 - \frac{h_1}{h_0} \right) h_0 + v_0^2}} \quad (15)$$

Transformation of Equation (15) with respect to h_1 leads to a cubic equation:

$$h_1^3 - \left(h_0 + \frac{v_0^2}{2g} \right) h_1^2 + \frac{Q^2}{2g(R\theta)^2} = 0 \quad (16)$$

$$h_1^3 - H_0 h_1^2 + \frac{1}{2g} \left(\frac{Q}{R\theta} \right)^2 = 0 \quad (17)$$

where: $H_0 = h_0 + \frac{v_0^2}{2g}$ = depth at the exit (cm).

To solve Equation (17), we reduce it to an "incomplete" form using the substitution

$$h_1 = x + \frac{H_0}{3} \quad (18)$$

The cubic equation with the new variable will look like this:

$$x^3 - 3 \left(\frac{H_0}{3} \right)^2 x - 2 \left[\left(\frac{H_0}{3} \right)^2 - \frac{1}{4g} \left(\frac{Q}{R\theta} \right)^2 \right] = 0 \quad (19)$$

According to Cardan's formula, the root of Equation (19) corresponding to the conditions of this problem will be:

$$x = -2 \frac{H_0}{3} \cos \left(60^\circ + \frac{\beta}{3} \right) \quad (20)$$

where: β = determined by the Equation (21):

$$\cos \beta = 1 - \frac{27}{4gH_0^3} \left(\frac{Q}{R\theta} \right)^2 = 1 - \frac{6.75}{\alpha_0} \left(\frac{h_{cr}}{H_0} \right)^3 \quad (21)$$

Then, from Equations (18) and (19), the formula for determining the depth before the jump is represented in the following form:

$$h_1 = \frac{H_0}{3} \left[1 - 2 \cos \left(60^\circ + \frac{\beta}{3} \right) \right] \quad (22)$$

The depth ratio h_1/h_0 in radical expression according to the law of continuity is:

$$\frac{h_1}{h_0} = \frac{v_0}{v_1} \frac{b_0}{R\theta} \quad (23)$$

$$\frac{h_1}{h_0} = \frac{v_0}{\sqrt{2g\left(1 - \frac{v_0}{v_1} \cdot \frac{b_0}{R\theta}\right)h_0 + v_0^2}} \frac{b_0}{R\theta} \quad (24)$$

The right-hand side of Equation (25) includes the velocity in the compressed section v_1 , which can be determined by the Equation:

$$v_1 = v_{np.1} = \sqrt{2g\left(1 - \frac{b_0}{R\theta}\right)h_0 + v_0^2} \quad (25)$$

where: $v_{np.1}$ = approximate value of the velocity in the compressed section ($\text{m}\cdot\text{s}^{-1}$).

In Equation (23), if $v_0 = v_1$, then the depth ratio h_1/h_0 can be expressed by the Equation (26):

$$\frac{h_1}{h_0} = \frac{b_0}{R\theta} \quad (26)$$

Taking into account Equations (23) and (25), we write the final form of Equation (15).

Obviously, the determination of h_1 according to Equation (26) can lead to some errors, then according to the following Equation (27), more reliable calculation values can be obtained, since the error caused by the assumption $v_0 = v_1$ turns out to be under the triple square root.

$$h_1 = \frac{Q}{R\theta \sqrt{2g\left[1 - \frac{b_0 v_0}{R\theta \sqrt{2g\left(1 - \frac{v_0}{v_{np.1}} \cdot \frac{b_0}{R\theta}\right)h_0 + v_0^2}}\right]h_0 + v_0^2}} \quad (27)$$

Thus, the use of Equations (9) and (22) or (27) makes it possible to set the limiting value of the depth in the diversion channel, the excess of which is accompanied by flooding of the hydraulic jump and the formation of new forms of conjugation of the pits.

The general procedure for the developed methodology for calculating the conjugate depths of a hydraulic jump is characterised as follows.

At the beginning of the calculation, the angle of spreading of the stormy flow in the plan is determined by the Equation (2). Then, the values of the radius of the arc along which the jump drum is outlined, R and the angle θ corresponding to the length of the drum line in the plan are calculated. Then, using Equations (22) or (27), the depth of the flow h_1 in the compressed section before the jump is determined. And the conjugate depths of the spatial jump are set by Equation (9).

RESULTS AND DISCUSSION

The results of calculations using the proposed method for calculating the conjugate depths of a hydraulic jump are shown in Table 1.

As can be seen from the table, when calculating the depth h_1 , the width of the jet from under the shield b_0 was disassembled in five variants (10; 12; 15; 17; 20 cm). Moreover, in the first four variants, the values of water supply were repeated within $(5-8)\cdot 10^3 \text{ cm}^3\cdot\text{s}^{-1}$, and in the fifth version they were 9 and $10 \text{ cm}\cdot\text{s}^{-1}$.

Experiments to verify the results of theoretical research were carried out, as indicated above, on a glass tray at values of $\eta = 0.4-0.8$ shows a view of a hydraulic jump formed during a symmetric planned compression of the flow at the initial moment of flooding with water with the formation of a drum at the left side of the chute (Photo 2).

Comparison of the obtained calculated values of h_1 using Equations (9), (22), (27) and the selection method (baseline) show that the greatest coincidence with the baseline value occurs when calculating by Equation (27) (deviation 0.15–0.21%). This is due to the fact that this formula takes into account almost all technological components that affect the initial action of a hydraulic jump.

Table 1. Results of calculations using the proposed method ($b_p = 42 \text{ cm}$)

Q ($\text{cm}^3\cdot\text{s}^{-1}$)	b_0 (cm)	h_0 (cm)	h_1 (cm) calculated acc. to			
			selection method	Equation (9)	Equation (22)	Equation (27)
$5\cdot 10^3$	10	5.56	0.796	0.807	1.168	0.795
$6\cdot 10^3$	10	6.28	0.898	0.930	1.319	0.838
$7\cdot 10^3$	12	6.16	1.067	1.071	1.153	1.068
$8\cdot 10^3$	12	6.74	1.168	1.064	1.696	1.167
$5\cdot 10^3$	15	4.25	0.930	0.933	1.326	0.933
$6\cdot 10^3$	15	4.80	1.054	1.037	1.511	1.054
$7\cdot 10^3$	17	4.89	1.230	1.253	1.662	1.231
$8\cdot 10^3$	17	5.34	1.345	1.359	1.907	1.346
$9\cdot 10^3$	20	5.18	1.562	1.550	2.177	1.564
$10\cdot 10^3$	20	5.56	1.675	1.676	2.336	1.676

Explanations: Q = water consumption ($\text{cm}^3\cdot\text{s}^{-1}$), b_0 = inlet flow width (cm), h_0 = flow depth in the outlet section 0–0 (cm), h_1 = depth at the beginning of the hydraulic jump (cm).

Source: SHINIBAEV [2010].

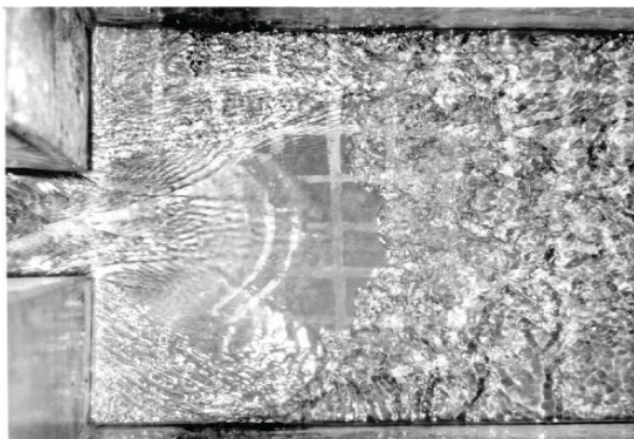


Photo 2. View of a spatial hydraulic jump at the beginning of flooding (phot. A. Shinibaev)

At the same time, as can be seen from the photo, the type of jump on the section with the greatest spreading of the stormy stream is outlined along a curve close to the arc of a circle with a radius determined by the Equation (28):

$$R = \frac{b_p}{2\sin\alpha} \quad (28)$$

where: b_p = width of the structure channel.

In general, the experimental results show that with an increase in the compression ratio (a decrease in b_o/b_p), the length of the section with a malfunctioning narrowing of a quiet flow increases.

With a compression ratio of $\eta \leq 0.5$, the extreme streams coming from the edges of the entrance are intertwined. Due to this, oblique waves are formed within the limits of the constriction, and the motion is qualitatively different from the cases when $\eta > 0.5$. When the angle of expansion is within $7-10^\circ$, a malfunctioning flow of a turbulent flow is observed, which has high kineticity at a distance from the outlet section of the structure.

With an increase in the water depth in the downstream, the flow at the junction section is more and more corrected in plan. At an angle of $25-27^\circ$, the flow is calm, the unevenness of the velocity distribution along the width of the channel (flume) is weakly expressed. It has been established that, in addition to the above-considered form of a spatial jump behind structures with $b_p/b_o > 3-4$, there can be another type of jump, which forms immediately behind the outlet of a structure without preliminary planned spreading of a stormy stream. A characteristic feature of such a jump is that the lateral vortex areas are flooded and the depth h_o in the outlet section is less than the critical depth in the outlet channel.

A decrease in the head and depth in the discharge channel would lead to the formation of a section with free or semi-free spreading of a stormy stream and a jump with a roller curved in plan behind it. When the jump, which forms behind the spreading section, is flooded, a new form of conjugation of flows arises, which is called the "malfunctioning flow".

Table 2 shows a comparison of the results of calculations of conjugate depths using the proposed method with experimental data. At $h_{cr}/h_o < 1.2$, at times, the formation of a wavy jump with a malfunctioning flow of a stormy stream is possible and the value of the drum length is unstable. The maximum deviation from the measured value is within acceptable limits, 2.35–4.54%.

Table 2. Comparison of calculation results using the proposed method ($b_p = 42$ cm)

Q (cm ³ ·s ⁻¹)	b_o	h_o	h_{cr}	R	h_1	h_{2cal}	h_{2exp}
	cm						
$4.25 \cdot 10^3$	16.6	3.51	4.13	33.58	0.91	4.19	4.00
$8.17 \cdot 10^3$	16.6	5.43	6.68	33.50	1.42	6.51	6.60
$11.30 \cdot 10^3$	16.6	6.37	7.92	35.29	1.75	8.09	7.90
$5.07 \cdot 10^3$	13.0	4.71	5.54	33.07	0.93	5.02	4.90
$8.45 \cdot 10^3$	13.0	6.53	7.68	33.07	1.32	7.01	6.80
$12.30 \cdot 10^3$	13.0	8.39	9.87	33.07	1.69	9.05	8.80

Explanations: b_p = width of the structure channel (cm), b_o = inlet flow width (cm), h_o = flow depth in the outlet section 0–0 (cm), h_{cr} = critical water depth in a curved section, R = jet deflection radius (cm), h_{2cal} = calculated depth values at the end of the hydraulic jump (cm); h_{2exp} = experimental depth values at the end of the hydraulic jump (cm); Q = water consumption (cm³·s⁻¹), h_1 = depth at the beginning of the hydraulic jump (cm).

Source: SHINIBAEV [2010].

CONCLUSIONS

The developed formulas in the theoretical study of the process make it possible to determine the limiting value of the flow depth in the outlet channel, the excess of which is accompanied by the flooding of the spatial jump and the formation of new forms of conjugation of the bays.

Some danger for erosion, the downstream support behind the water regulating structure is a malfunctioning flow of a calm stream when the compression ratio of the structure in the plan is equal to or less than 0.5, and the depth in the downstream is more critical.

At an angle of expansion within $7-10^\circ$, a faulty flow of a turbulent flow is observed, which has a high kineticity at a distance from the outlet section of the structure. With an increase in the water depth in the lower reaches, the flow at the butt section is more and more corrected in plan. At an angle of $25-27^\circ$ the current is calm, the unevenness of the velocity distribution along the width of the channel (chute) is weakly expressed.

For forced expansion of the flow at the outlet of the water control structure in critical cases, it is recommended to use additional energy absorbers.

ACKNOWLEDGMENTS

We are grateful for the target program of the Ministry of Education and Science of the Republic of Kazakhstan "Development and improvement of water treatment technology and improvement of the quality of drinking water in the regions of Kazakhstan" (BR 11765599, KazNITU), which allowed us to complete this work.

REFERENCES

- ABBASPOUR A., TAGHAVIANPOUR T., ARVANAGHI H. 2019. Experimental study of the hydraulic jump on reverse bed with porous screens. Applied Water Science. Vol. 9(7) p. 1–7. DOI 10.1007/S13201-019-1032-7.

- ABDURAMANOV A. 2010. *Gidravlika [Hydraulics]*. Taraz. Senim. ISBN 978-5-91327-515-8 pp. 497.
- ASHOOR A., RIAZI A. 2019. Stepped spillways and energy dissipation: A non-uniform step length approach. *Applied Water Science*. Vol. 9(23). DOI 10.3390/app9235071.
- BEGLYAROVA E.S., BAKSHANIN A.M., DMITRIEVA A.V., SOKOLOVA S.A., MIKHAILET D.P. 2018. Eksperimental'nyye issledovaniya zatoplenogo gidravlicheskogo pryzhka v neprizmaticheskom rusle pryamougol'nogo secheniya pri gladkom gorizonta'lnom dneksperimental studies of a submerged hydraulic jump in a non-prismatic rectangular bed with a smooth horizontal bottom]. *Prirodoobustroystvo*. No. 3 p. 51–57. DOI 10.26897/1997-6011/2018-3-51-58.
- BEIRAMI M., CHAMANI M. 2006. Hydraulic jumps in sloping channels: Sequent depth ratio. *Journal of Hydraulic Engineering*. Vol. 132 (10) p. 1061–1068.
- BOUSSEKINE V., LAKHDAR DJEMILI L. 2016. Modelling approach for gravity dam break analysis. *Journal of Water and Land Development*. No. 30 p. 29–34. DOI 10.1515/jwld-2016-0018.
- CANILHO H., FAEL C. 2018. Velocity field analysis of a channel narrowed by spur dikes to maximize power output of in-stream turbines. *Journal of Sustainable Development of Energy, Water and Environment Systems*. Vol. 6(3) p. 534–546. DOI 10.13044/j.sdwes.d6.0197.
- CARVALHO P., SPATARU C., BLEISCHWITZ R. 2019. Integration of water and energy planning to promote sustainability. *Journal of Sustainable Development of Energy, Water and Environment Systems*. Vol. 7(2) p. 229–252. DOI 10.13044/j.sdwes.d6.0246.
- CLOPPER P., LAGASSE P. 2011. Hydrologic uncertainty in prediction of bridge scour. Final report. Transportation Research Board. Vol. 2262(1) p. 207–213. DOI 10.3141/2262-21.
- DANIEL R.A., PAULUS T.M. 2019. Managing accidents and failures of hydraulic structures, *MATEC Web of Conferences*. Vol. 284, 08003 p. 3–7. DOI 10.1051/mateconf/201928408003.
- DE LEO A., RUFFINI A., POSTACCHINI M., COLOMBINI M., STOCCHINO A. 2020. The effects of hydraulic jumps instability on a natural river confluence: The case study of the Chiaravagna River (Italy). *Water (Switzerland)*. Vol. 12(7) p. 1–18. DOI 10.3390/w12072027.
- EL-ASKARY W.A., NASR M., ABDEL-FATTAH A. 2013. Study of turbulent flow in rectangular channel with inclined baffles. *Journal of Fluid Mechanics*. Vol. 731(6) p. 25–32. DOI 10.21608/erjm.2009.69434.
- EL-HAZEK A.N., ABDEL-MAGEED N.B., HADID M.H. 2020. Numerical and experimental modelling of slope stability and seepage water of earthfill dam. *Journal of Water and Land Development*. No. 44 p. 55–64. DOI 10.24425/jwld.2019.127046.
- ERSOY S.R., TERRAPON-PFAFF J., RIBBE L., MERROUNI A.A. 2021. Water scenarios modelling for renewable energy development in Southern Morocco. *Journal of Sustainable Development of Energy, Water and Environment Systems*. Vol. 9(1) p. 1–28. DOI 10.13044/j.sdwes.d8.0335.
- EEA 2020. Water availability, surface water quality and water use in the Eastern Partnership countries. An indicator-based assessment. EEA Report. No. 14. Copenhagen. European Environment Agency. ISBN 978-92-9480-291-0 pp. 74. DOI 10.2800/635170.
- FRIZELL K.W., FRIZELL K.H. 2015. Guidelines for the hydraulic design of stepped spillways. Hydraulic Laboratory Report HL-2015-06. Denver. U.S. Dept. of the Interior, Bureau of Reclamation pp. 39.
- JONES J.S., RICHARDSON E.V. 2004. A decade of high priority bridge scour research in the U.S. [online]. In: *Proceedings 2nd International Conference on Scour and Erosion*. Eds. Y.-M. Chiew, S.-Y. Lim, N.-S. Cheng. 14–17.11.2004 Singapore. Vol. 1 p. 105–110. [Access 10.01.2021]. Available at: https://henry.baw.de/bitstream/handle/20.500.11970/99972/PAS_3.pdf?sequence=1&isAllowed=y
- KASHEFIPOUR S.M., BAKHTIARI M. 2009. Hydraulic jump in a gradually expanding channel with different divergence angles [online]. 33rd IAHR Congress: Water Engineering for a Sustainable Environment (IAHR) p. 91–98. [Access 10.01.2021]. Available at: <https://rms.scu.ac.ir/Files/Articles/Conferences/Abstract/10180.pdf200910404950250.pdf>
- KASSYMBEKOV ZH.K., SHINIBAEV A.D. 2009. Issledovaniye razmerov promyvnoy voronki za mnogoproletnym shlyuzom-regulyatorom v zavisimosti ot sostoyaniya potoka [Study of the dimensions of the flushing funnel behind the multi-span sluiceregulator, depending on the state of the flow]. *Materialy mezhdunarodnoj konferencii "Perspektivy razvitiya nauki i tekhniki"*. Prague p. 22–30.
- LEMOULT G., AIDER J. L., WESFREID J.E. 2013. Turbulent spots in a channel: Large-scale flow and self-sustainability. *Journal of Fluid Mechanics*. Vol. 731 p. 1–12. DOI 10.1017/JFM.2013.388.
- MIKHALEV M.A. 2013. Modeling of channel erosion downstream spillway dams. *Magazine of Civil Engineering*. Vol. 37 p. 67–74. DOI 10.5862/MCE.37.10.
- MICHALOLIAS N., KERAMARIS E., KASITEROPOULOU D., LIAKOPOULOS A., PECHLIVANIDIS G. 2018. Experiments and numerical analysis of flow in an open channel with gravel bed. *Proceedings*. Vol. 2(11), 581. DOI 10.3390/proceedings2110581.
- OMID M.H., ESMAEELI V.M., NARAYANAN R. 2007. Gradually expanding hydraulic jump in a trapezoidal channel. *Journal of Hydraulic Research*. Vol. 45(4) p. 512–518. DOI 10.1080/00221686.2007.9521786.
- REPETTO R., TUBINO M., PAOLA C. 2002. Planimetric instability of channels with variable width. *Journal of Fluid Mechanics*. Vol. 457 p. 79–109. DOI 10.1017/S0022112001007595.
- RUSTIATI N.B., DERMAWAN V., RISPININGTATI, LIMANTARA L.M. 2017. The influence of sandy clay bed material to local scour behavior. *Journal of Water and Land Development*. No. 35 p. 193–202. DOI 10.1515/jwld-2017-0084.
- SADIQ S.M. 2007. Characteristics of the hydraulic jump in trapezoidal channel section. *The Journal of Environmental Studies (JES)*. Vol. 9 p. 53–63.
- SHEPPARD D.M., ODEH M., PRITSIVELIS A., GLASSER T. 2004. Clearwater local scour experiments in a large flume. DOI 10.1061/40517(2000)130.
- SHINIBAEV A.D. 2010. Issledovanie i predotvrashchenie lokal'noj erozii na otkrytyh vodoreguliruyushchih ob'ektah vodosnabzheniya [Investigation and prevention of local erosion at open water regulation facilities of the water supply system]. Abstract of PhD Thesis. Almaty. Satbayev University pp. 41.
- SUTHERLAND S.H., SMITH B.T. 2018. Resilience Implications of Energy Storage in Urban Water Systems. *Journal of Sustainable Development of Energy, Water and Environment Systems*. Vol. 6(4) p. 674–693. DOI 10.13044/j.sdwes.d6.0210.
- TREBICKA A. 2018. Efficiency and optimum decisions using the simulation of water distribution system. *Journal of Ecological Engineering*. Vol. 19(6) p. 254–258. DOI 10.12911/22998993/89832.
- TSKHAI A.A., AGEIKOV V.Y. 2021. Disturbance of sustainability of the reservoir ecosystem: A model approach for assessing and forecasting the long-term process of eutrophication. *Journal of Sustainable Development of Energy, Water and Environment Systems*. Vol. 9(1) p. 1–16. DOI 10.13044/j.sdwes.d8.0327.

- WU J., CHEN J., HAN Y., LI T. 2020. Study on unsteady flow based on optimized water distribution model in irrigation district. *Sustainability*. Vol. 12(4). DOI 10.3390/su12041580.
- XIA H., FRENKIEL F.N. 2017. Two-dimensional turbulence in three-dimensional flows. *The Physics of Fluids*. Vol. 29(5) p. 64–70. DOI 10.1063/1.5000863.
- ZHANG Q., XIA Q., LIU C.K. GENG S. 2013. Technologies for efficient use of irrigation water and energy in China. *Journal of Integrative Agriculture*. Vol. 12(8) p. 1363–1370. DOI 10.1016/S2095-3119(13)60544-4.
- ZHURINOV M., KASSYMBEKOV ZH.K., KASSYMBEKOV G.ZH. 2019. Mastering and development hydropower in Kazakhstan. *News of the Academy of Sciences of the Republic of Kazakhstan. Kazakh National Research Technical University named after K.I. Satpayev. Series of Geology and Technical Sciences*. Vol. 3. No. 435 p. 219–224. DOI 10.32014/2019.2518-170X.88.
- ZHURINOV M., KASSYMBEKOV ZH.K., DYUSSEMBEKOVA N., SIEMENS E., KASSYMBEKOV G.ZH. 2020. Testing of the prototype of mini-hydro power plants of hydrocyclone type in production conditions. *News of the Academy of Sciences of the Republic of Kazakhstan. Kazakh National Research Technical University named after K.I. Satpayev. Series of Geology and Technical Sciences*. Vol. 1. No. 439 p. 48–55. DOI 10.32014/2020.2518-170X.6.